Effect of residual stress on the tensile loading of a gradient microstructure material obtained by surface mechanical attrition treatment

Zihao Guo, Jianqiang Zhou, Bruno Guelorget, Zhidan Sun, Delphine Retraint, Benoît Panicaud

EFFECT OF RESIDUAL STRESS ON THE TENSILE LOADING OF A GRADIENT MICROSTRUCTURE MATERIAL OBTAINED BY SURFACE MECHANICAL ATTRITION TREATMENT

Zihao Guo[a,*], Jianqiang Zhou[b], Bruno Guelorget[a], Zhidan Sun[a], Delphine Retraint[a] and Benoît Panicaud[a]

[a] *LASMIS, Université de Technologie de Troyes (UTT), Troyes 10000, France*
[b] *School of Mechanical Engineering, Northwestern Polytechnical University, 710072, Xi'an, China*

ABSTRACT
During the surface mechanical attrition treatment (SMAT), residual stress, work hardening and grain nano-crystallization are produced simultaneously, which allows to enhance the mechanical properties of materials. In this work, a dislocation density-based constitutive model is adapted to describe the local mechanical behavior of the gradient microstructure generated by SMAT and predict the macroscopic behavior of a SMATed cylindrical structure under tensile loading. A finite element (FE) model is built to perform uniaxial tensile simulation with the introduction of a residual stress field and a work hardening gradient obtained by X-ray diffraction (XRD). The results of simulation are in good agreement with the experimental results. Furthermore, it has been found that the residual stress plays a significant role in the initial stage of deformation. It decreases the yield stress of such gradient microstructure materials.

Keywords: Gradient microstructure material; Residual stress; Surface mechanical attrition treatment; Tensile loading; Finite element modeling

1. Introduction

Surface Mechanical Attrition Treatment (SMAT) is based on multi-directional impacts on the surface of a material with shot boosted by an ultrasonic generator [1,2]. The severe plastic deformation due to the remarkably increased strain and strain rate can produce a great number of microscopic defects, which progressively induces nano-crystallization in the superficial layer of materials. However, SMAT cannot affect the metallurgical features and mechanical properties in the bulk material. Hence, a gradient microstructure is generated from the treated surface to the bulk with continuously increased grain sizes [3–5].

In the literature, various techniques such as Electron backscatter diffraction (EBSD), nano-indentation and X-ray diffraction (XRD), are widely used to investigate the morphological features and properties of gradient microstructure materials [6–8]. However, it is difficult for experimental investigations to precisely characterize the mechanical properties at different depths, especially for the nanocrystallized layer. Therefore, in the literature, theoretical modeling is implemented to investigate the microscopic mechanical performances. For instance, a mechanism-based strain gradient plasticity model was modified to describe the mechanical response of gradient microstructure materials [9–11]. In another work, the Kocks-Mecking-Estrin (KME) model was employed to describe the evolution of dislocation density with plastic strain rate and gradient grain size [12].

* Corresponding author. zihao.guo@utt.fr

Besides the gradient microstructure, high compressive residual stresses are inevitably induced in the near-surface region. The impacts also generate a gradient work hardening region, which could also have a significant effect on the mechanical behavior of materials [3]. In most work, the generated residual stresses are not considered in modeling, and only the work hardening gradient is taken into account through a dislocation density distribution [13]. In order to numerically and accurately investigate the mechanical properties of the gradient microstructure generated by SMAT, the residual stress and work hardening should be considered in the modelling.

This work aims thus to study the effect of residual stress on the properties of the gradient microstructure. For this purpose, the gradient microstructure of a SMATed 316L stainless steel is considered using a dislocation density and grain size based constitutive model. A 2D-axisymmetric cylindrical structure is built to analyze the uniaxial tensile mechanical behavior. Both the equilibrated residual stresses and the initial dislocation density distribution are implemented in the FE structure through user-defined subroutines.

2. Material and SMAT

2.1. Gradient microstructure obtained by SMAT

In this work, a dumbbell shape specimen of 316L stainless steel is treated on the entire gauge area, and the SMAT conditions are presented in a previous work [7]. As illustrated in Fig.1, a gradient microstructure can be observed on the cross-section of a SMATed specimen through EBSD. The microstructure manifests a clear gradient feature from a nanocrystallized layer at the top treated surface to a coarse-grained microstructure in the bulk region. Due to the multi-directional severe plastic deformation induced by the impacts of flying balls, the grain size is refined and it ranges from 50 nm to 300 nm within a superficial nanocrystallized layer with a thickness of 5 μm.

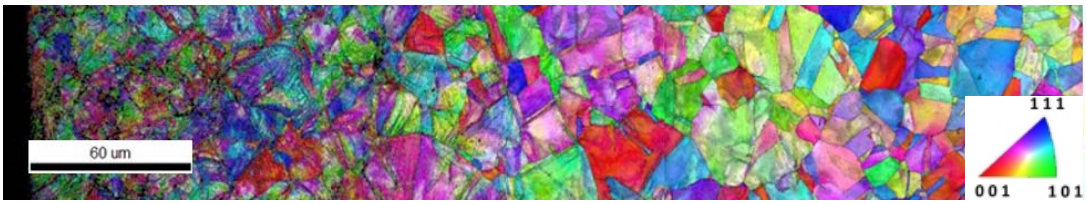

Fig. 1. Microstructure observation on the cross-section of the SMATed specimen.

2.2. Measurement of residual stress and work hardening

After the specimen was treated by SMAT, residual stresses and work hardening were measured by XRD. Work hardening cannot be directly measured, and it is usually evaluated by microscopic features (such as plastic slip and dislocation density). Iterative electrolytic polishing was performed to obtain their in-depth distributions in the near-surface region of the SMATed specimen [14]. The data points shown in Fig. 2a present the in-depth distribution of two residual stress components, respectively in the axial and circumferential directions. It can be seen that these two residual stresses exhibit compressive nature with a depth until about 500 μm. These residual stresses profiles will be taken into account in the further modeling.

As highlighted in Fig. 1, a large near-surface region is mechanically affected by SMAT due to high strain rate impacts. During the treatment, plastic strain is gradually accumulated in the near-surface region. In previous work [14], the residual accumulated plastic strain ε_{rs}^{p}, which can describe the extent of work hardening, was assessed from FWHM of XRD peaks by Eq. (1). The obtained in-depth distribution of ΔFWHM is shown in Fig. 2b.

$$\varepsilon_{rs}^{p} = \alpha \cdot \Delta FWHM \qquad (1)$$

$$\Delta FWHM = \begin{cases} 2.35(r_{\max} - r - 0.68)^2 \\ 0, \quad where \quad r < r_{\max} - 0.68 \end{cases} \tag{2}$$

where r and r_{max} are the distance to the axis of the cylindrical structure and the radius of the specimen, respectively; α is a coefficient of proportionality; $\Delta FWHM$ is the variation of FWHM between SMATed and untreated samples.

An equilibrium method for reconstruction of the residual stress field and the work hardening gradient is used in a cylindrical structure by FE modelling [14]. According to the elastic-plastic equilibrium and boundary conditions, the residual stresses and work hardening are recalculated to obtain the true residual stress field inside a cylindrical structure.

a b

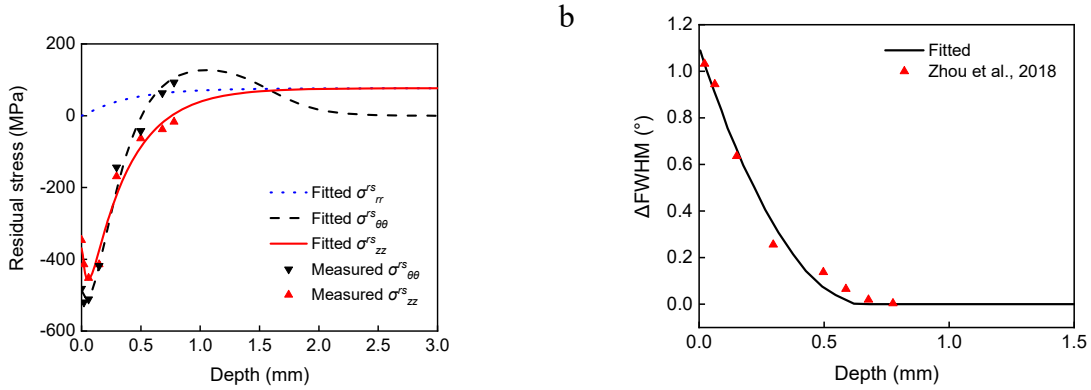

Fig. 2. In-depth distribution of (a) residual stress, and (b) ΔFWHM whose fitted curve based on Eq. (2) is given.

3. Modelling of gradient microstructure materials

3.1. Constitutive model

In the framework of elastic-viscoplastic model, the total strain rate tensor $\dot{\varepsilon}_{ij}$ can be decomposed into elastic and plastic parts:

$$\dot{\varepsilon}_{ij} = \dot{\varepsilon}^e_{ij} + \dot{\varepsilon}^p_{ij} \tag{3}$$

The elastic part obeys the linear relationship between elastic strain rate and stress rate defined by Hooke's model:

$$\dot{\varepsilon}^e_{ij} = \frac{1}{2\mu}\dot{\sigma}'_{ij} + \frac{\dot{\sigma}_{kk}}{9K}\delta_{ij} \tag{4}$$

where $\dot{\sigma}'_{ij} = \dot{\sigma}_{ij} - \frac{1}{3}\dot{\sigma}_{kk}\delta_{ij}$ is the deviatoric stress rate, $\dot{\sigma}_{kk}$ is the hydrostatic stress rate, δ_{ij} is the Kronecker's symbol; μ and K are the shear modulus and bulk modulus, respectively. The plastic strain rate tensor is related to the deviatoric stress $\sigma'_{ij} = \sigma_{ij} - \frac{1}{3}\sigma_{kk}\delta_{ij}$ based on the J2-flow theory of plasticity:

$$\dot{\varepsilon}^p_{ij} = \frac{3\dot{\varepsilon}^p}{2\sigma_e}\sigma'_{ij} \tag{5}$$

where $\dot{\varepsilon}^p = \sqrt{\frac{2}{3}\dot{\varepsilon}^p_{ij}\dot{\varepsilon}^p_{ij}}$ and $\sigma_e = \sqrt{\frac{3}{2}\sigma'_{ij}\sigma'_{ij}}$ are the equivalent plastic strain rate and the von Mises effective stress, respectively. In order to calculate without employing higher order stresses, a power law viscoplastic model [9] is used to determine the effective plastic strain rate:

$$\dot{\varepsilon}^p = \dot{\varepsilon}_0 \left[\frac{\sigma_e}{\sigma_{flow}}\right]^m \tag{6}$$

where *m* (larger than 20) is the rate-sensitivity exponent; $\dot{\varepsilon}_0$ is a reference strain rate; σ_{flow} is the flow stress. According to Taylor's hardening model and Hall–Petch strengthening [15,16], the flow stress in the gradient microstructure materials can be described as:

$$\sigma_{flow} = \sigma_0 + \frac{k_{HP}}{\sqrt{d}} + M\alpha\mu b\sqrt{\rho} \tag{7}$$

where σ_0 is the lattice friction stress; k_{HP} is the Hall-Petch slope; *d* is the grain size; *M* is the Taylor factor; α is a material constant ; μ is the shear modulus; b is the magnitude of Burger's vector of the material ; ρ is the dislocation density. A modified KME model is employed to represent the evolution of the dislocation density. Moreover, an additional dynamic recovery term is added to decrease the work hardening due to grain refinement:

$$\frac{\partial\rho}{\partial\varepsilon^p} = M\left[\frac{k_0}{bd} + \frac{k_1}{b}\sqrt{\rho} - k_{20}\left(\frac{\dot{\varepsilon}^p}{\dot{\varepsilon}_0}\right)^{-\frac{1}{n_0}}\rho - \left(\frac{d_e}{d}\right)^2\rho\right] \tag{8}$$

where k_0 and k_1 are geometric factors related to grain boundary and dislocation forests; k_{20} is the dynamic recovery constant; n_0 is an exponent inversely proportional to temperature; d_e is the reference grain size.

3.2. Grain size distribution

As indicated in Section 2.1, the grain size varies from nanometric at the top treated surface to micrometric in the non-affected bulk region. This grain size distribution should be included in the finite element model. Based on experimental results reported in the literature [6,7], an exponential relationship is adopted to describe the variation of grain size in the gradient microstructure:

$$d = d_0 10^{k_d z} \tag{9}$$

where *z* is the distance from the treated surface; $k_d = \lg(d_c / d_0)/h_g$, with h_g being the thickness of the gradient grain size layer; d_0 and d_c are the grain size of the topmost surface and the one of the non-affected bulk region, respectively. The material parameters which describe the gradient grain size are provided in Table 1.

Table 1. Material parameters for gradient grain size [7].

Symbol	d_0 (nm)	d_c (μm)	h_g (μm)
Value	50	20	550

3.3. Dislocation density distribution

As presented in Section 2.2, the work hardening induced by SMAT was assessed through measuring FWHM by XRD. As a consequence, the residual accumulated plastic strain ε_{rs}^p was calculated based on ΔFWHM (Eq. (1) and (2)). It is well documented that there is a link, to some extent, between accumulated plastic strain and dislocation density, and models were proposed previously in the literature [17,18] to calculate dislocation density based on measured accumulated plastic strain. In this work, the initial dislocation density is related to the residual accumulated plastic strain through the following equation:

$$\rho_0 = 2\sqrt{3}\frac{(\varepsilon_{rs}^{p2})^{\frac{1}{2}}}{bd} \tag{10}$$

As shown in Fig. 3, the initial dislocation density (based on Eq. (10)) and the accumulated plastic strain decrease gradually from the treated surface to the bulk region. The decrease rate is lower as the depth increases. It can also be seen that this distribution is consistent with the data points presented by Ghosh et al. [18].

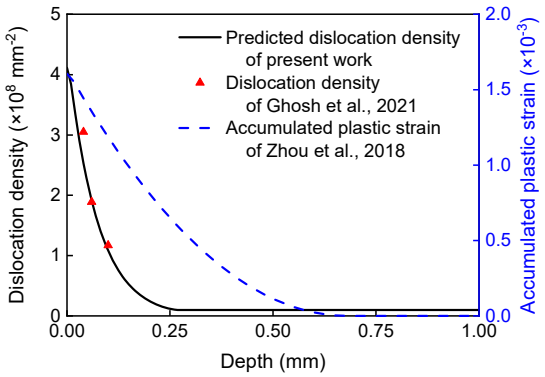

Fig. 3. In-depth distribution profile of initial dislocation density and accumulated plastic strain. The data points obtained from the literature are also given.

3.4. Reconstruction of residual stress field

The residual stress profiles are measured using XRD, as shown in Fig. 2a. These profiles should be implemented in the finite element structure. As presented in previous work [14], exponential functions based on the stress equilibrium conditions are built to describe the in-depth distribution of residual stress:

$$\begin{cases} \sigma_{zz}^{rs} = \sum_{i=1}^{2} L_i \left(e^{-l_i (r_{\max} - r)} \right) + L_0 \\ \sigma_{\theta\theta}^{rs} = \sum_{i=1}^{2} T_i \left(e^{-t_i (r_{\max} - r)} \right) + T_0 \\ \sigma_{rr}^{rs} = \frac{1}{r} \left[\sum_{i=1}^{2} \frac{T_i}{t_i} \left(e^{-t_i (r_{\max} - r)} - 1 \right) - T_0 \left(r_{\max} - r \right) \right] \end{cases} \quad (11)$$

where L_0, L_i, l_i, T_0, T_i and t_i are constant and fitted from the residual stress profiles presented in Fig. 2b. Table 2 lists the values of the parameters involved in Eq. (11).

We can obtain the residual stress components distribution, as shown in Fig. 2a. It can be seen that the maximum compressive stress values are at the near-surface region for both axial and circumferential components. It should be noted that tensile residual stress, which occurs in the bulk region, is present to insure the equilibrium of the whole structure.

Table 2. The parameters of residual stress reconstruction model.

Axial					Circumferential				
L_1 (MPa)	l_1	L_2 (MPa)	l_2	L_0 (MPa)	T_1 (MPa)	t_1	T_2 (MPa)	t_2	T_0 (MPa)
10547.64	6.95	-11303.32	6.19	188.58	315.23	17.36	-832.24	2.84	91.60

4. Finite element simulation

4.1. The model with initial variables and fields

A 2D-axisymmetric model is built to analyze the tensile properties of gradient microstructure materials. In order to build a complete model of gradient microstructure materials, the residual stresses are introduced as initial state at the beginning of simulation through the user-defined subroutine SIGINI. The grain size and initial dislocation density are compiled as functions

implemented into the subroutine UMAT with an elastic-viscoplastic behavior. Material parameters for the model are defined in Table 3. Two analysis steps are performed for the procedure, including a self-equilibrium analysis and followed by a tensile simulation. The residual stress and work hardening distributions are introduced and balanced during the first step.

Table 3. Parameters for the model of gradient microstructure materials.

Symbol	σ_0 (MPa)	K_{HP} (MPa·m$^{1/2}$)	M	A	μ (GPa)	b (nm)
Value	70 [1]	0.25 [1]	3.06 [9]	0.3 [9]	82	0.256 [9]
Symbol	k_0	k_1	k_{20}	n_0	ϵ_0 (s^{-1})	de (μm)
Value	0.1 [9]	0.026	2.5	21.25 [9]	1 [9]	20 [7]

After implementing the finite element model, the distribution of each variable can be verified. It can be observed in Fig. 5a that the yield stress significantly increases with grain size. In the nanostructured layer, the stress level can reach about 1560 MPa, whereas the value in the bulk region is only about 190 MPa. This is due to the fact that the grain boundary strengthening effect can significantly improve the yield strength of the gradient microstructure materials (see Eq. (7)). It shows that there is a good agreement between the calculated curve and these experimental points. The implemented grain size distribution can be found in Fig. 5b. The grain size varies from 50 nm at the top surface to 20 μm in the bulk region based on Eq. (9).

a b

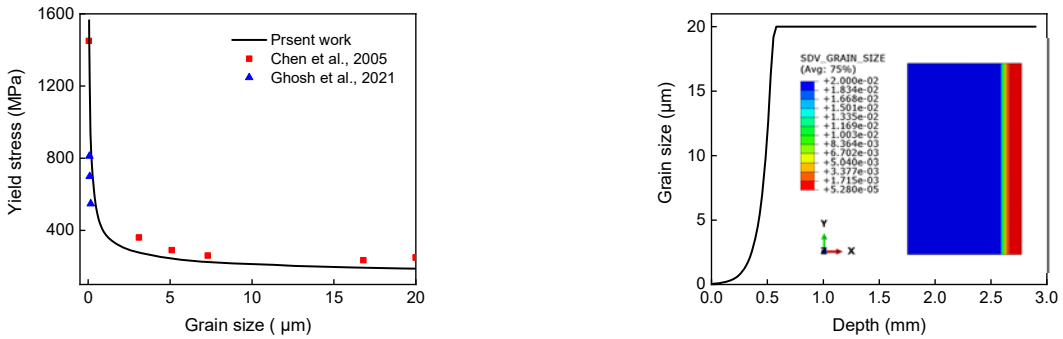

Fig. 5. In-depth distribution profiles of (a) yield stress; (b) grain size.

4.2. Results and discussion

4.2.1. Mechanical behavior of gradient microstructure materials

In order to compare the local mechanical behavior of the gradient microstructure, four representative depths associated with grain sizes corresponding to 50 nm, 200 nm, 1 μm and 20 μm are chosen to illustrate the stress-strain curves under uniaxial tension loading. For comparison, the simulated stress-strain curve of gradient microstructure with residual stress is also given by dash curves in Fig. 6. It can be observed that the residual stress mainly influences the mechanical behavior in the initial stage of deformation. Moreover, the presence of compressive residual stresses delays the occurrence of plastic deformation, which is more significant in the nanocrystallized layer.

4.2.2. Evolution of dislocation density with strain

Fig. 7 shows the evolution of equivalent plastic strain and dislocation density during tensile loading for the materials with different grain sizes, i.e. at different depths. It can be found that the equivalent plastic strain increases with the imposed strain for all the grain sizes, i.e. in the whole structure (both SMAT affected and bulk regions). Note that the equivalent plastic strain

remains constant during the elastic deformation stage. Except for the nanocrystallized layer (Fig. 7d), the dislocation density increases and its increase can be associated with the equivalent plastic strain (see Fig. 7a-c). The phenomenon of dislocation density reduction shown in Fig. 7d can be attributed to the dynamic recovery of dislocations due to work hardening effect in the nanocrystallized layer, as mention in Eq. (8).

By referring to the residual stress profiles presented in Fig. 2a, it can be seen that the residual stress has a small influence on the evolution of equivalent plastic strain and dislocation density (see dashed curves in Fig.7).

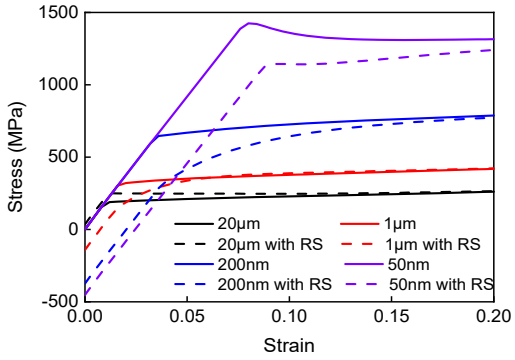

Fig. 6. The simulated stress-strain curves of different grain sizes with and without residual stress (RS).

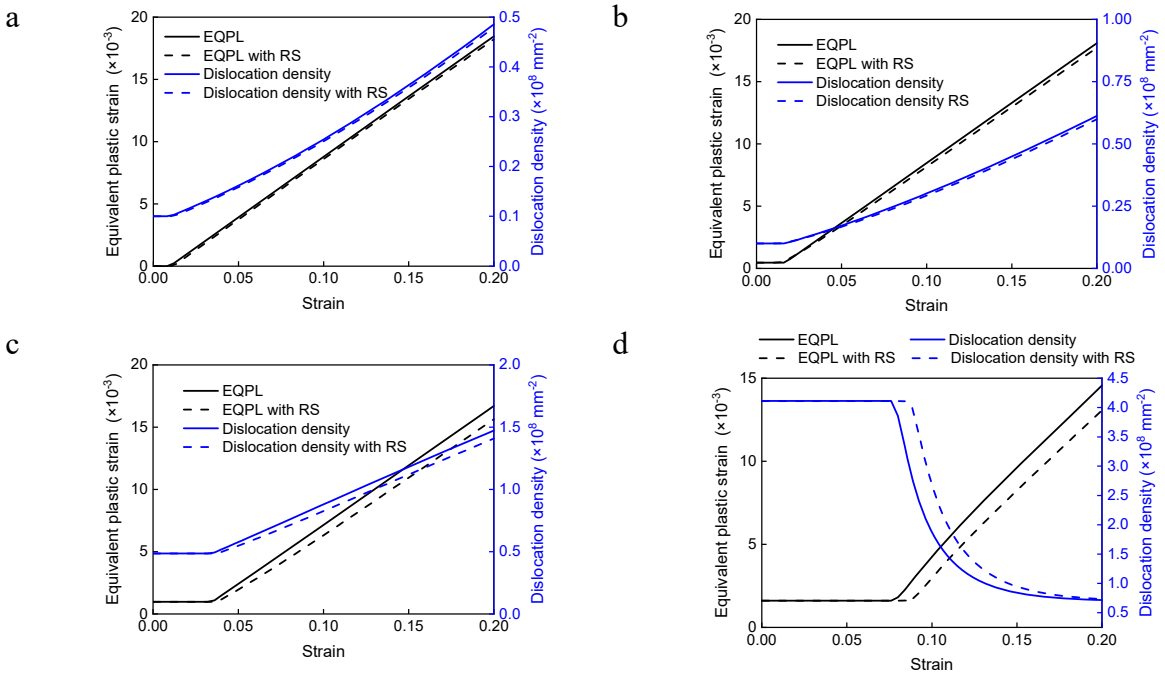

Fig. 7. Evolution of equivalent plastic strain (EQPL) and dislocation density of gradient microstructure with and without residual stress (RS). The grain sizes are: (a) 20 μm; (b) 1 μm; (c) 200 nm; (d) 50 nm.

5. Conclusions

In this study, a dislocation density-based model is adapted to investigate the tensile behavior of gradient microstructure materials by taking into account the residual stress and the grain size. Based on the obtained results, the following conclusions can be drawn:

- By comparing the tensile stress-strain curves of gradient materials with different grain sizes (i.e. at different depths), it can be found that the residual stress plays a significant role in the initial stage of deformation. Moreover, the compressive residual stress delays the occurrence of plastic deformation especially in the very near surface region (with grain sizes of 50 nm and 200 nm).

- In the region far from the surface (with grain sizes of 1 μm and 20 μm), the residual stress has a small influence on the evolution of equivalent plastic strain and dislocation density, whereas in the very near surface region, this influence is more pronounced.

6. Acknowledgements

Z. Guo greatly appreciates the financial support from the China Scholarship Council (CSC).

References

[1] X. H. Chen, J. Lu, L. Lu, and K. Lu, Tensile properties of a nanocrystalline 316L austenitic stainless steel, Scripta Materialia, 52 (2005) 1039–1044.
[2] K. Lu and J. Lu, Nanostructured surface layer on metallic materials induced by surface mechanical attrition treatment, Materials Science and Engineering: A, 375 (2004) 38–45.
[3] H. W. Huang, Z. B. Wang, J. Lu, and K. Lu, Fatigue behaviors of AISI 316L stainless steel with a gradient nanostructured surface layer, Acta Materialia, 87 (2015) 150–160.
[4] Y. B. Lei, Z. B. Wang, B. Zhang, Z. P. Luo, J. Lu, and K. Lu, 'Enhanced mechanical properties and corrosion resistance of 316L stainless steel by pre-forming a gradient nanostructured surface layer and annealing', Acta Materialia, 208 (2021) 116773.
[5] G. Liu, J. Lu, and K. Lu, Surface nanocrystallization of 316L stainless steel induced by ultrasonic shot peening, Materials Science and Engineering: A, 286 (2000) 91–95.
[6] T. H. Fang, W. L. Li, N. R. Tao, and K. Lu, Revealing Extraordinary Intrinsic Tensile Plasticity in Gradient Nano-Grained Copper, Science, 331 (2011) 1587–1590.
[7] Y. Wu, B. Guelorget, Z. Sun, R. Déturche, and D. Retraint, Characterization of gradient properties generated by SMAT for a biomedical grade 316L stainless steel, Materials Characterization, 155 (2019) 109788.
[8] F. Yin et al., Strain rate sensitivity of the ultrastrong gradient nanocrystalline 316L stainless steel and its rate-dependent modeling at nanoscale, International Journal of Plasticity, 129 (2020) 102696.
[9] J. Li and A. K. Soh, Modeling of the plastic deformation of nanostructured materials with grain size gradient, International Journal of Plasticity, 39 (2012) 88–102.
[10] J. Zhao et al., Multiple mechanism based constitutive modeling of gradient nanograined material, International Journal of Plasticity, 125 (2020) 314–330.
[11] L. Zhu, H. Ruan, A. Chen, X. Guo, and J. Lu, Microstructures-based constitutive analysis for mechanical properties of gradient-nanostructured 304 stainless steels, Acta Materialia, 128 (2017), 375–390.
[12] U. F. Kocks and H. Mecking, Physics and phenomenology of strain hardening: the FCC case, Progress in Materials Science, 48 (2003) 171–273.
[13] Z. Chen, Z. Sun, and B. Panicaud, Investigation of ductile damage during surface mechanical attrition treatment for TWIP steels using a dislocation density based viscoplasticity and damage models, Mechanics of Materials, 129 (2019) 279–289.
[14] J. Zhou, Z. Sun, P. Kanouté, and D. Retraint, Reconstruction of residual stress and work hardening and their effects on the mechanical behaviour of a shot peened structure, Mechanics of Materials, 127 (2018) 100–111.
[15] B. P. Kashyap and K. Tangri, On the Hall-Petch relationship and substructural evolution in type 316L stainless steel, Acta Metallurgica et Materialia, 43 (1995) 3971–3981.
[16] G. I. Taylor, The mechanism of plastic deformation of crystals. Part I.—Theoretical, Proc. R. Soc. Lond. A, 145 (1934) 362–387.
[17] G. K. Williamson and R. E. Smallman, III. Dislocation densities in some annealed and cold-worked metals from measurements on the X-ray debye-scherrer spectrum, Philosophical Magazine, vol. 1 (1956) 34–46.
[18] S. Ghosh, N. Bibhanshu, S. Suwas, and K. Chatterjee, Surface mechanical attrition treatment of additively manufactured 316L stainless steel yields gradient nanostructure with superior strength and ductility, Materials Science and Engineering: A, 820 (2021) 141540.